



Toward Surreptitious Remote Sensing of Blood Alcohol Concentration: Results with Integrated Near-Infrared Spectral Imaging and Laser Speech Detection

Peer review status:

No

Corresponding Author:

Dr. Robert Lodder,
Professor, Pharmaceutical Sciences, BPC223 Biopharmaceutical Complex, 40536 - United States of America

Submitting Author:

Dr. Robert Lodder,
Professor, Pharmaceutical Sciences, BPC223 Biopharmaceutical Complex, 40536 - United States of America

Other Authors:

Dr. Thaddaeus Hannel,
Chemistry, University of Kentucky - United States of America

Dr. David Link,
Chemistry, University of Kentucky - United States of America

Article ID: WMC005185

Article Type: Research articles

Submitted on: 29-Sep-2016, 03:00:12 AM GMT **Published on:** 01-Oct-2016, 10:39:46 AM GMT

Article URL: http://www.webmedcentral.com/article_view/5185

Subject Categories: ALCOHOLISM

Keywords: molecular factor computing, integrated sensing and processing, BrAC, BAC, interferometer

How to cite the article: Lodder R, Hannel T, Link D. Toward Surreptitious Remote Sensing of Blood Alcohol Concentration: Results with Integrated Near-Infrared Spectral Imaging and Laser Speech Detection. WebmedCentral ALCOHOLISM 2016;7(10):WMC005185

Copyright: This is an open-access article distributed under the terms of the [Creative Commons Attribution License \(CC-BY\)](#), which permits unrestricted use, distribution, and reproduction in any medium, provided the original author and source are credited.

Source(s) of Funding:

This work was supported in part by the NIH under NIAAA N01AA 33003, DARPA, and KSEF (Grant #KSEF-914-RDE-008), and by the National Center for Research Resources and the National Center for Advancing Translational Sciences, National Institutes of Health, through Grant UL1TR000117. The content is solely the responsibility of the authors and does not necessarily represent the official views of the NIH.

Competing Interests:

No competing interests.

Toward Surreptitious Remote Sensing of Blood Alcohol Concentration: Results with Integrated Near-Infrared Spectral Imaging and Laser Speech Detection

Author(s): Lodder R, Hannel T, Link D

Abstract

Alcohol abuse is a major problem in the United States. The most common measurement tool used in law enforcement for the determination of alcohol concentration in subjects is the breath analyzer (BrAC), and subjects know when they are being measured. However, when surreptitious measurements of BrAC in freely moving humans are sought, then hyperspectral remote-sensing measurement techniques must be used. In this work, two remote sensing methods for the estimation of BrAC were studied. A clinical trial involving human subjects was performed to assess the supposition that molecular factor computing (MFC) near-infrared (NIR) hyperspectral imaging and speech analysis using laser interferometry could be used to noninvasively estimate BrAC in subjects at a distance. A conventional breath analyzer was used to provide reference measurements. MFC NIRS imaging measurements gave a standard error of prediction (SEP) for a global model (all subjects) for blood alcohol of 8.1 mg/dL (0.0081%) and $r^2 = 0.987$. The laser interferometer measurements of speech gave an average SEP for individual subject results for blood alcohol of 9.0 mg/dL (0.0090%) and $r^2 = 0.975$.

Introduction

The problem of alcohol abuse

The abuse of alcohol (ethanol) is a major problem in the United States for health and economic reasons. More than 125 million Americans aged 12 or older are alcohol consumers¹. Alcohol abuse has long been known to lead to heart and liver problems, increased risk-taking behavior, and reduction of ability to operate a motor vehicle¹. According to the National Traffic Highway Safety Administration's Fatality Analysis Reporting System (FARS), in 2012, 33.8% percent of all auto crash fatalities were the result of alcohol impairment². The problems arising from the abuse of alcohol are not limited to the road and affect the

well-being of many Americans. Alcohol has been shown to lower inhibitions and increase risk-taking behavior¹. In 2001, over 1,700 alcohol-related unintentional deaths occurred among college students, and there were approximately 696,000 assaults by students who had been drinking³. Economically, alcohol abuse harms entire communities, costing taxpayers huge amounts of money spent in order to protect them from those who are abusing alcohol. The total yearly economic cost of alcohol abuse in 1998 was estimated to be 184.6 billion dollars⁴.

Treatments for abusers of alcohol, including Alcoholics Anonymous (AA) and other behavior modification-style organizations, are easy to find. However, the bulk of alcohol-related problems are caused by individuals who are not seeking help. Approximately 39 percent of the 400,000 Americans admitted to alcohol treatment programs are there due to a court order and not by personal choice⁵. The need to remain alcohol-free in order to remain free from incarceration provides an incentive for individuals to lie about their consumption to counselors and parole officers. A similar problem arises for the scientific community studying the effects of alcohol treatment programs. Evaluating treatments requires a continuous monitor of subjects' blood alcohol content (BAC), breath alcohol content (BrAC, known to be highly correlated to BAC⁶), or actual consumption. Current alcohol content monitoring techniques include the sampling of breath, urine, saliva, or blood followed by a different analysis to assess the alcohol level in each. Blood testing is the most sensitive method, but the test can suffer from temporal distortion due to the processing time needed to obtain the result. Samples can ferment on their own over time, leading to inaccurate measurements of alcohol consumption. Temporal distortion is problematic in the research setting when a time-sensitive result is needed. Urine testing is perhaps the most inexpensive of the techniques, but it tests for alcohol in the system in the past five days, not in real-time⁷. Techniques that integrate consumption over long periods of time can complicate experiments designed to test the effects of treatment on acute alcohol abuse. Contamination, dilution, and tampering

with the samples are other common problems in urine testing⁷⁻⁸. Breath analyzers are the most common on-site monitoring technique and are generally used by law enforcement on the public. The breath analyzer is the only noninvasive technique that can be used to monitor real-time alcohol levels, but it has many drawbacks. Some breath analyzer devices assume a hematocrit (cell volume of blood) of approximately 47 percent, when in reality it ranges from 37 to 52 percent⁹. Testing an individual with a hematocrit level below the assumed value will result in a false positive reading on the breath analyzer⁹. Breath testing can also lead to false positives when blood, alcohol, or vomit is present in an individual's mouth.

One approach to monitoring alcohol abuse is through the use of wristband fuel cells or implants that record a series of alcohol levels. The use of the Secure Continuous Remote Alcohol Monitoring (SCRAM) system has become common for those convicted of DUI. The SCRAM device monitors transdermal alcohol content (TAC) in the body. The SCRAM is attached to the offender's ankle for typically a period of a month. However, problems have been noted with use of the SCRAM device. An offender placed in an alcohol supervision program that uses a SCRAM device may not use any products such as mouthwash or household cleaners that contain alcohols, because these products can cause the device to produce a false positive. The device monitors attempts to bypass it by monitoring body temperature. If a sudden temperature change is recorded at the detector, an alert will be sent to the monitor. A problem with all monitoring methods discussed so far is that the subject is aware that he or she is being monitored, enabling the subject to attempt to defeat the device.

A noninvasive and surreptitious measurement of BrAC is of interest because of the many problems regarding the existing real-time and more intrusive methods. If a subject is unaware of when the measurement is being made, it becomes more difficult to attempt to defeat the measurement. Illustration 1 depicts the use of MFC-NIR hyperspectral imaging and laser speech detection for unobtrusive monitoring of a subject. The engineering design scenario is formulated on a grill & bar restaurant and remote sensing. Envision several people sitting around a table inside the grill & bar. Everyone has a drink or two in front of them as well as some food. The objective is to determine the BrAC of each person sitting at the table (without anyone knowing they are being measured) from a vehicle located outside the restaurant in the parking lot. NIR hyperspectral imaging may be used to estimate the BrAC using diffuse reflectance from the skin of the

people sitting at the table. NIR laser interferometry may sense vibrations in the glasses of the individuals sitting around the table as they speak, and use these vibrations to record their speech. As with NIR hyperspectral imaging, the BrAC may also be estimated from the way in which people speak. This paper describes experiments to estimate BrAC using NIR hyperspectral imaging based on high throughput molecular factor computing (a method of integrated sensing and processing) and speech analysis. These approaches have the potential to estimate alcohol impairment unobtrusively, remotely, and in real-time.

Near-Infrared (NIR) Imaging

NIR spectroscopy has been demonstrated to be a valuable analytical tool for the simultaneous determination of multiple chemical components in mixtures. As a result, NIR spectroscopy is used throughout the biotechnology and pharmaceutical industries¹⁰⁻¹⁵. Pulse oximetry, a medical application of NIRS, is very common in hospitals¹⁶. The NIR region of the electromagnetic spectrum offers advantages for use in biological systems. NIR radiation is able to penetrate through the dermal layers of skin and has been shown to measure accurately blood levels of analytes *in vivo*¹⁷⁻¹⁸. Thus, diffuse reflectance NIR imaging is a candidate for noninvasive determination of blood alcohol. The combination of NIR imaging with molecular factor computing (MFC) filters offers several advantages over the traditional approach to NIR imaging¹⁹. Advantages of using an MFC filter system with NIR imaging include a decrease in computational demand by integrating the sensing and processing directly into the transducer (the integrated sensing and processing, or ISP, advantage), the Fellgett advantage (acquisition of all wavelengths simultaneously permits higher signal-to-noise ratio for a given acquisition time), and the Jacquinot advantage (the absence of monochromator slits allows higher optical throughput). The use of a small number of MFC filters also allows for a more robust instrument at a lower cost. The concept of molecular factor computing has been demonstrated in previous work²⁰.

NIR hyperspectral imaging creates large volumes of data because images are acquired over many wavelengths where the analyte is expected to have signals. Most images also contain a substantial number of pixels, and many images are often collected to form a video stream. The data sets generated by hyperspectral imaging can be difficult to analyze. To this end, chemometric methods such as factor analysis are commonly used to reduce large data sets into factors and corresponding weights that relate to the observed variance in the data set. MFC-NIR

hyperspectral imaging exploits these chemometric methods and can be an effective alternative to conventional hyperspectral imaging^{12,21-22}. MFC essentially incorporates chemometrics directly into the physical design of the wavelength selector, thus integrating the sensing and processing at the detector itself^{20,23}. MFC filters are selected to have transmission spectra that match the weights generated from factor analysis of a calibration set. Thus, the light passing through a MFC filter is effectively "weighted", and the corresponding signal at the detector is proportional to a factor. The use of weighted filters allows for factor analysis to be performed at the speed of light. The chemometric method we have used to perform MFC is principal component analysis (PCA).

Illustration 2 illustrates the use of MFC filters. A theoretically perfect MFC filter would have a transmission spectrum that perfectly matches a positive or negative loading profile of the sample. In most cases, a perfect MFC filter cannot be constructed. In cases where a perfect MFC filter cannot be constructed, partially modeling a PC loading may still give acceptable results. In previous work, liquid filters were used to determine ethanol and water concentrations²⁰. In this work, solid polymer filters were used that were composed of non-alcoholic functional groups. To design a set of polymer filters, a set of training spectra is collected from ethanol consumers over many wavelengths. Principal component loadings reveal spectral regions where variation in analyte concentration is greatest. Molecular factor (MF) filters are selected to closely match a loading profile. Because MF filters cannot have negative responses, two MF filters are required. A broadband source is used to illuminate a target and the reflected light is passed through the MF filter. Only wavelengths corresponding to regions where spectral variability is greatest can pass through the filter. Because the MF filter is chemometrically weighted, the voltage response at the detector is proportional to the analyte sought.

Speech Analysis

Determination of BrAC using speech is based on changes in phonemes that occur after consumption of alcohol. It has been shown that an individual's speaking fundamental frequency changes with alcohol consumption²⁴. Language comprises various sounds—the smallest units that define spoken word are known as phonemes²⁵. In the United States, the English language consists of approximately 44 phonemes²⁵. While the number of phonemes in other languages is different from English, some speech changes would

still be expected to be associated with alcohol consumption. Speech can be recorded surreptitiously and remotely, and there are various instruments made for this purpose, such as parabolic microphones (Dan Gibson Parabolic Microphone, Electromax International, Inc. Houston, Texas) used in television and broadcasting. However, there are other less obtrusive methods available for monitoring speech. A laser microphone-listening device outside of a building, such as the one offered by Brinkhouse Security (New York, NY), could be used to remotely monitor conversations inside a building, as long as glass windows are present in the building walls. Using a laser microphone method, law enforcement personnel could monitor conversation inside a restaurant, bar, or car, making determinations of which patrons are over the legal limit for BAC. As the patrons went to their car and left, they could be stopped by police.

The following work describes preliminary research to determine which remote-sensing modalities can provide sensitive and specific detection of BrAC.

Experimental

Patient Screening

The unobtrusive remote-sensing of human breath alcohol content study was conducted under IRB-approved protocols (approval number 07-0417-F1V).

NIRS MFC Hyperspectral Imaging

An IRC-160 InSb focal plane array video camera (Cincinnati Electronics, Mason, OH) with molecular factor computing (MFC) filters was used for imaging of the patients. The camera integration time was 12.96 ms, and the photon energy response was 1800-10,000 cm⁻¹. A rotating disk was fabricated to allow the different MFC filters to be rotated in front of the camera lens. Six filter materials were used for the study: polyvinyl chloride (PVC, Unbranded, McMaster-Carr), polycarbonate (PC, Lexan, Plaskolite, Inc.), Acrylic (AC, Unbranded), polymethyl-methacrylate (PMA, Optix, Plaskolite, Inc.), combined gel filters CC20B and CC40G (BG, Kodak), and Gel A2 Pale Yellow (A2, Kodak). The light source was two 250W PC37771 lamps (General Electric, Cleveland, OH). Chemicals for the MFC filters were chosen using a genetic algorithm library search. In previous work, liquid filters were selected with the algorithm from a library of NIR transmission spectra containing 1,923 compounds (Wiley)²⁰. The genetic algorithm searched the database for up to ten compounds that provided a combined transmission

spectrum that closely resembled a factor loading. The spectral library available for this research was composed of liquids, which would be harder than polymer filters to deploy in a clinical trial. For this reason, a smaller list of available polymers was ultimately used to create the MFC filters. Selecting from a smaller database of available filters limits the performance of the MFC hyperspectral imager somewhat. However, solid polymer filters make the system more rugged and easier to use in the field.

Subjects were never in exactly the same position for measurements. To compensate for changes in image contrast and intensity resulting from subject position changes and variable illumination over the acquisition period, pictures of two spherical silicon dioxide reflectance standards²⁶ (one high reflectance and one low reflectance) were captured in each image. Images in the video stream were made comparable by multiplicative scatter correction^{27, 21} based on the reflectance standards, so that the standards appeared identical throughout all images. A flat image reference standard (Kodak Gray Card, Rochester, NY) was also used to correct for temporal and spatial inconsistencies in detector response across the pixels of the detector array. Two light sources were employed during image acquisition to reduce shadowing and increase the signal-to-noise ratio of the data. The lights were placed on each side of the camera and approximately 135 degrees relative to an orthogonal line connecting the patient and camera lens. Images were obtained with each MFC filter with the light sources turned off and with them on (12 total spectral images) to correct for ambient lighting from the room and blackbody radiation from the patient. The entire video acquisition process took only 2 minutes.

Laser Speech Instrumentation

The remote speech detection instrumentation was fabricated in-house and was based on Michelson interferometry. The interferometer utilized a battery-powered laser pointer (635 nm) as the source to simplify aiming. (Production versions will use an invisible laser wavelength within the range of the NIR camera to enable aiming.) The interference fringe pattern was detected with a phototransistor and amplifier using a soundcard (M-Audio, Avid Technology Inc) and was recorded into Cool Edit Pro (Syntrillium Software Corp.) at a sample rate of 44.1 kHz. The laser beam was aimed at a glass target positioned 2 to 3 feet from each patient. The sound from patients' speech induced vibrations in the glass causing constructive and destructive interference patterns at the phototransistor, which were amplified

and recorded. The changes in the interference patterns were stronger at frequencies where the glass target had resonances. A unidirectional microphone (ECM-330, Sony) that lacked the resonances of the glass was also used as a reference and placed next to the reflecting glass. This reference was used ad hoc to estimate the resonances of the remote glass. The test subjects were given a list of 13 words to read (table, flat, feet, pet, light, bit, bone, hot, future, thumb, boot, soil, saw) containing common phonemes in the English language.

Data Analysis

Analytical software was written in MatLab 7.1 (The Mathworks, Inc.). Principal component analysis (PCA)²⁸ was used to analyze all data except for MFC voltage data. The multivariate regression method was cross-validated in predicting BrAC using both NIR MFC images and speech data. The F test and the standard error of performance (SEP) were calculated from the validation samples²⁹⁻³⁰.

The NIRS video consisted of indexed color images with a resolution of 72 pixels/inch and dimensions of 720x480 pixels (width by height). The images were imported into MatLab 7.1 where a matrix of intensity levels with a size of 720x480x3 (rows by columns by dimensions) was created. The dimensions corresponded to the red, green, and blue (RGB) color space where the color intensities for a specific pixel were combined to give 1 of 256 possible colors³¹. The subject's face fit the vertical length of the image and was constant. However, horizontal movement of the subject's face throughout the testing period could not be avoided. Therefore it was necessary to crop portions of the subject's face because of movement, dead areas in the frame, and areas where the signal-to-noise ratio was very low due to highly reflecting materials such as hair. Each subject's face was cropped in four areas: forehead, under the eyes, and lower face as depicted in illustration 3. In some cases the use of lower face data was prevented by facial hair, and forehead data was limited where the subject had low hanging hair. The cropped images were separated into three layers representing RGB, then gray and multiplicative scatter correction was performed. To determine if the voltage corresponded to a PC score, each color layer of the cropped images was averaged to produce a single voltage score. Multivariate regression was performed on the voltage data from each cropped facial region. All possible combinations of three, four, and five MFC filters of the total six were used to determine if a correlation existed. Because the MFC filters were not perfectly weighted functions of the ethanol in humans, PCA and

multivariate regression was also performed on the filter data. Leave-one-out cross-validation was used to determine the prediction ability of the model for BrAC values from NIRS imaging.

Cool Edit Pro was used to apply noise reduction to the microphone speech data only. This was done by creating a noise profile for each patient. The noise profile was created by sampling the background noise in the audio track (i.e. before the subject began speaking). The background noise sample was applied to the full waveform with the noise reduction option using a FFT size of 12000 and a precision factor of 10^{32} . The data were imported into MatLab following noise reduction. The speech data were analyzed in two ways: analysis was completed on full phrases (i.e., all words together in sequence) and on individual words. To accomplish this, the time domain data were cropped so that there was one data set for all combined words and one data set for each of the 13 words spoken by each subject. All time domain data were Fourier transformed into the frequency domain. PCA was applied to all data sets and multivariate analysis was used to determine if correlations between speech and BrAC existed. All multivariate models were validated using leave-one-out cross-validation.

Results and Discussion

NIR Image Data

The purpose of the MFC filter is to increase S/N and reduce the numeric processing associated with an analytical method. In theory, if the MFC filters had been perfectly weighted functions of the ethanol in humans, the resulting intensity signals at each pixel of the images would be proportional to ethanol concentration in blood and no other calculations would need to be made. In this case there were six MFC filters that yielded six pseudo PC scores (voltage scores). Calculation of the voltage scores from the MFC filters required sampling several pixels at different facial regions, as described previously. The pixels were averaged together for each image and used as the single voltage score for the corresponding filter. This produced one data point per image per filter. In the end there were six voltage scores for each sample concentration. However, this analysis did not produce highly correlated results probably due to the imperfect nature of the filters as factor loadings and the introduction of noise from patient movement. For example, as described in illustration 2, two filters are required for each PC loading used. The MFC filters used in this experiment represented only the positive loadings. Illustration 4 indicates the r^2 values from

each subject using multivariate regression and leave-one-out cross validation for MFC image data. The standard error of prediction (SEP) for the correlations in illustration 4 can be found in illustration 5.

Principal components and multivariate regression were performed combining all combinations of colors (RGB) and MFC filters together to find the best correlation. The regression correlations and cross-validation statistics for each subject from a full facial profile that mathematically describe the fitness of the model and the prediction ability of the model for BrAC values from PCA of MFC NIR imaging is indicated in illustrations 4 and 5. Post-processing factor scores (i.e., 6 scores instead of ca. 1000 wavelengths) by PCA gave the best results. Image data were assembled together from all patients to make a pooled global calibration for testing the prediction ability when the subject is unknown (i.e., not previously calibrated). Illustration 6 A. indicates the global model predicted BrAC with $r^2 = 0.987$ and $SEP = 0.0081 \% \text{ BrAC}$.

Speech Spectral Data

The time domain data were Fourier transformed (FT) into the frequency domain. The FT was performed such that every frequency became a data point from the sample (sampling rate = 44.1 kHz, therefore each sample was a 1×22050 matrix). All spaces in the time domain data not containing speech were removed so that the FT was a combination of all frequencies of speech instead of other sounds. Due to the large volume of data, PCs were calculated over a limited frequency interval where speech was expected to be found. Frequency differences were observed among the different phonemes associated with the words used in this study. Illustration 7 shows the speech spectra from patient 5 obtained from the interferometer and microphone for words "boot" and "light". The interferometer captured lower frequencies similar to that of the microphone. However, it was found that the microphone captured higher frequency signals with a much better S/N ratio. As a result, the laser interferometer produced speech spectra that showed BrAC correlations with frequencies lower than those observed in the microphone spectra. This preference for lower frequencies in the interferometer data was attributed to audio frequency resonances in the reflecting glass. Due to the nature of the recording device and room noise, the signal to noise (S/N) ratio of the laser interferometer was lower than the microphone. The average frequency range associated with BrAC correlations to interferometer-recorded speech was 150 to 900Hz. The laser interferometer-recorded speech spectra produced individual

correlations with $r^2 > 0.91$ and $SEP < 0.017\%$ BrAC. Illustrations 8 and 9 depict the r-square and SEP statistics respectively, from multivariate regression and leave-one-out cross-validation observed for each word. An $r^2 = 0.806$ and $SEP = 0.017\%$ BrAC was found for the average pooled interferometer spectral data. The relatively poor performance of the global model is most likely due to the small sample size ($n=5$) and may be attributed to the differences in individual vocal clarity and ability. Hollien et al. noted that differences in fundamental frequency are found between men and women²⁴.

The microphone-recorded speech spectra produced individual correlations to BrAC of $r^2 > 0.95$ and $SEPs < 0.015\%$ BrAC. Illustrations 10 and 11 illustrate the microphone-recorded r-square and SEP statistics respectively, from multivariate regression and leave-one-out cross-validation. The average frequency range associated with BrAC correlations to microphone-recorded speech was 150 to 1050 Hz. A global model was calculated by pooling the microphone speech spectra for each word. An $r^2 = 0.805$ and $SEP = 0.016\%$ BrAC was found for the average pooled microphone spectral data. Illustration 6 B and C illustrates the prediction capability for the global speech model for spoken words bit (interferometer recorded) and boot (microphone recorded), respectively. Again, the relatively poor performance of the global model is most likely due to the small sample size ($n=5$) and because of differences in vocal characteristics of each patient.

Conclusion

MFC-NIR hyperspectral imaging and speech are shown to correlate with BrAC. MFC-NIRS imaging returned a global correlation much higher ($r^2 = 0.987$, $SEP = 0.0081\%$) than that of the speech detection method. Although the predictions made from principal component regression of the MFC filter data were somewhat better than predictions made from the voltage data alone, the results suggest that MFC may be capable of producing a more robust prediction. The MFC filters used in this research were selected from a small database of available materials. The number of filter materials available for MFC is high and better methods of filter selection may be needed for MFC to be a more useful technique. There may also be a market for production of solid state filters for MFC-NIR hyperspectral imaging. The advantages of MFC-NIR hyperspectral imaging over traditional NIR hyperspectral imaging include a decrease in the computational demand, shorter acquisition and

analysis times, and higher signal-to-noise ratio. MFC also has the advantage of increased optical throughput because many wavelengths are acquired at the same time.

Problems with determining the portions of the patient's face to analyze increased measurement noise lead to a less accurate prediction model. This problem may be fixed by incorporating an algorithm to distinguish between exposed skin and hair (hair is highly reflective in the NIR).

Speech results for individual calibrations were shown to correlate well with BrAC. Laser microphone-listening devices can be expensive, but we have shown it is possible to build a device for less than \$100. The global model for speech determination of BrAC is more difficult to find than for hyperspectral imaging. However, the results of this study suggest that individual calibrations of speech can allow for its use in commercial industries.

MFC-NIR hyperspectral imaging and laser speech detection complement each other in freely moving humans, because a face may not always be visible, and speech may not always be available. MFC-NIR hyperspectral imaging and laser speech detection may be of use to law enforcement for noninvasive alcohol monitoring of subjects. However, due to the ethical and constitutional dilemmas posed by this research, noninvasive alcohol monitoring may find better use in alcohol treatment.

REFERENCES

1. <http://www.drugabusestatistics.samhsa.gov/NSDUH/2k6NSDUH/2k6results.cfm#Ch3>, checked 10/27/2014.
2. <http://www.fars.nhtsa.dot.gov/>, checked 10/27/2014.
3. NIH Publication No. 07-5010, http://www.collegedrinkingprevention.gov/1College_Bulletin-508_361C4E.pdf, checked 10/27/2014.
4. NIH, <http://pubs.niaaa.nih.gov/publications/economic-2000/index.htm#updated>, checked 10/27/2014.
5. Drug and Alcohol Services Information System, <http://www.oas.samhsa.gov/2k5/alcTX/alcTX.htm>, checked 10/27/2014.
6. Jones, AW Beylich, KM Bjorneboe, A Ingum J and Morland, *J Clinical Chemistry* 38: 743-747, 1992.
7. Rouen, David; Dolan, Kate. A Review of Drug Detection Testing and an Examination of Urine, Hair, Saliva and Sweat. National Drug and Alcohol

- Research Centre. ISBN 0-7334-1790-6 (2001).
8. Katz, N. Fanciullo, GJ. Role of urine toxicology testing in the management of chronic opioid therapy. *Clin J Pain* 2002; 18:4.
9. Hlastala, Michael. The alcohol breath test-a review. *J. of Appl Physiol* 1998; 84:402-408.
10. Dempsey, R. J. Davis, D. G. Buice, R. G. and Lodder R. A.. Biological and medical applications of near-infrared spectroscopy. *Appl. Spectrosc.* 50:18A-34A (1996).
11. Drennen J. K. and Lodder R. A.. Nondestructive near-infrared analysis of intact tablets for determination of degradation products. *J. Pharm. Sci.* 79:622-627 (1990).
12. El-Hagrasy, A. S. Morris, H. R. Amico, F. D, Lodder, R. A. and Drennen, J. K. 3rd. Near-infrared spectroscopy and imaging for the monitoring of powder blend homogeneity. *J. Pharm. Sci.* 90:1298-1307 (2001).
13. Urbas, A. Manning, M. W. Daugherty, A. Cassis, L. A. and Lodder R. A. Near-infrared spectrometry of abdominal aortic aneurysm in the ApoE^{-/-} mouse. *Anal. Chem.* 75:3318-3323 (2003).
14. Ridder, T. D. Hendee, S. P. and Brown C. D.. Noninvasive alcohol testing using diffuse reflectance near-infrared spectroscopy. *Appl. Spectrosc.* 59:181-189 (2005).
15. Soto, J. C. Meza, C. P. Caraballo, W. Conde, C. Li, T. Morris, K. R. and Romanach. R. J. On line non-destructive determination of drug content in moving tablets using near infrared spectroscopy. *Journal of Process Analytical Technology* 2(5):8-14 (2005).
16. Ingram, G Munro; *N Br J Gen Pract.*, July 1; 55(516): 501-502, 2005.
17. **Malin, Stephen F. Ruchti, Timothy L. Blank, Thomas B. Thennadil Suresh N. and Monfre, Stephen L.** *Clinical Chemistry* 45: 1651-1658, 1999.
18. **Robinson, MR Eaton, RP Haaland, DM Koepp, GW Thomas, EV Stallard BR and Robinson, PL** *Clinical Chemistry* 38: 1618-1622, 1992.
19. Lyon, Robbe C. Lester, David S. Lewis, E. Neil Lee, Eunah Yu, Lawrence X. Jefferson Everett H. and Hussain, Ajaz S. *AAPS PharmSciTech*, 3 (3) article 17, 2002.
20. Dai, Bin Urbas, Aaron Douglas, Craig C. Lodder, Robert A. *Pharmaceutical Research*, 2007 DOI: 10.1007/s11095-007-9260-1.
21. Burger J.; Geladi P., Hyperspectral NIR image regression part I: Calibration and correction, *J. Chemometrics* 2005; 19: 355-363.
22. Cassis, Lisa A Urbas, Aaron Lodder Robert A ; *Analytical and Bioanalytical Chemistry*, Trends, 2004, DOI: 10.1007/s00216-004-2979-1.
23. Medendorp, Joseph Lodder, Robert A. J. *Chemometrics* 2005; 19: 533-542.
24. Hollien, H DeJong, G Martin, C. A. Schwartz, R. Liljegren; *K. J. Acoust. Soc. Am.*, Vol. 110, No. 6, December 2001.
25. Sousa, David A. How the Brain Learns to Read, Corwin Press, pp222, 2005.
26. Dempsey, Robert J. Davis, Daron G. Buice, Robert G. Jr., Lodder, Robert A. *Applied Spectroscopy*, Volume 50, Issue 2, Pages 18A-34A, 1996.
27. Isaksson T, Kowalski B. Piece-wise multiplicative scatter correction applied to near-infrared diffuse transmittance data from meat products. *Appl Spectrosc.*;47(6):702-709, 1993.
28. Miller, James N., Miller, Jane C., Statistics and Chemometrics for Analytical Chemistry 4th ed., Person Education Limited. 2000, 217-221.
29. Thomas, E. V.; Haaland, A. C. *Anal. Chem.* 1990, 62, 1091-1099.
30. Beebe, K. R.; Kowalski, B. R. *Anal. Chem* 1987, 59, 1007A-1017A.
31. Pratt, James. Digital Image Processing. 4th Ed. ISBN 978-0-471-76777-0, John Wiley & Sons (2007).
32. Adobe, <http://kb.adobe.com/selfservice/viewContent.do?externalId=332261&slicId=1>, checked 4/17/2010.

Illustrations

Illustration 1

Illustration 1



Illustration 1. Remote alcohol sensing. A hypothetical situation where (1) an NIR laser beam reflected from the glass on the table and interferometer are used to monitor speech as well as alcohol content of the beverage, and (2) MFC-NIR hyperspectral imaging is used for laser positioning and to determine the subject's BAC.

Illustration 2

Illustration 2

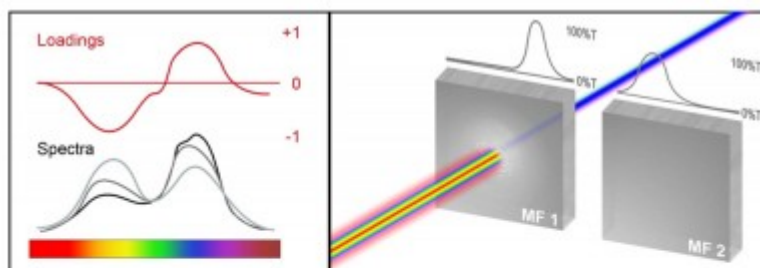


Illustration 2. A set of training spectra is collected over many wavelengths. Loadings correspond to spectral regions where variation in analyte concentration is greatest. Molecular factor (MF) filters are selected to closely match a loading profile. Because MF filters cannot have negative responses, two MF filters are required. A broadband source is used to illuminate a target and the reflected light is passed through the MF filter. Only wavelengths corresponding to regions where spectral variability is greatest can pass through the filter. Because the MF filter is chemometrically weighted, the voltage response at the detector is proportional to the analyte sought.

Illustration 3

Illustration 3

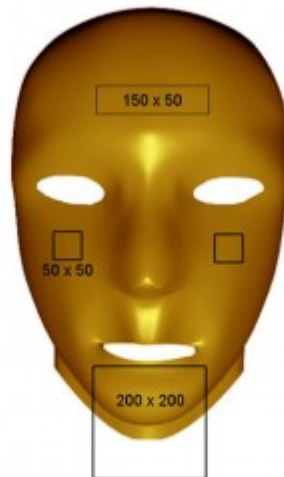


Illustration 3. To minimize artifacts due to movement of the subject over the acquisition period, four areas were focused on for each subject image: forehead, under the eyes, and lower face with horizontal and vertical areas indicated. The lower face region also included a portion of the subject's neck.

Illustration 4

Illustration 4

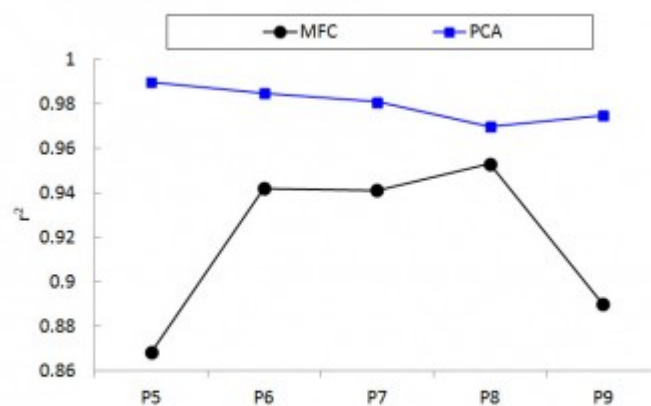


Illustration 4. Comparison of MFC and PCA image calibration results from leave-one-out cross-validation of actual versus predicted % BrAC. P5 – P9 indicate patient ID.

Illustration 5

Illustration 5

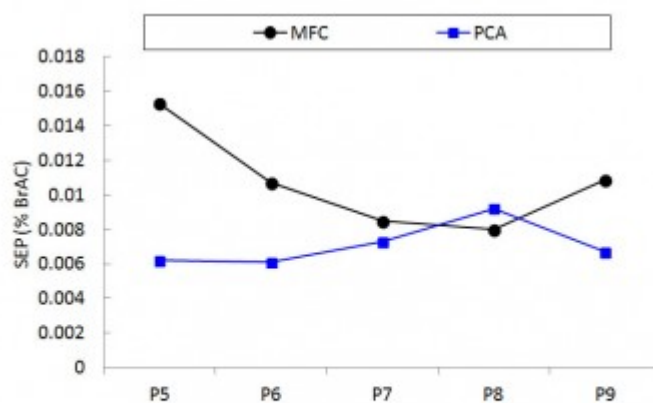


Illustration 5. Comparison of PCA and MFC image calibration SEP values for leave-one-out cross-validation of actual versus predicted % BrAC. P5 – P9 indicate patient ID.

Illustration 6

Illustration 6

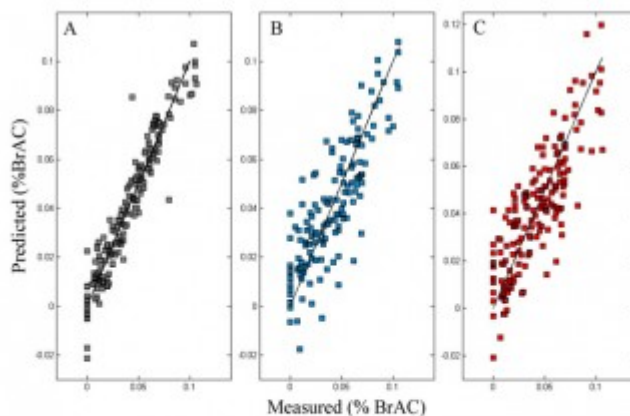


Illustration 6. Global calibration plots of predicted % BrAC versus the actual % BrAC using leave-one-out cross validation based on A: PCA of MFC NIR image data: $r^2 = 0.987$ and SEP = 0.0081 % BrAC. B: Interferometer recorded speech for word "bit": $r^2 = 0.852$ and SEP = 0.0153 % BrAC. C: Microphone recorded speech for word "boot": $r^2 = 0.8432$ and SEP = 0.0151 % BrAC.

Illustration 7

Illustration 7

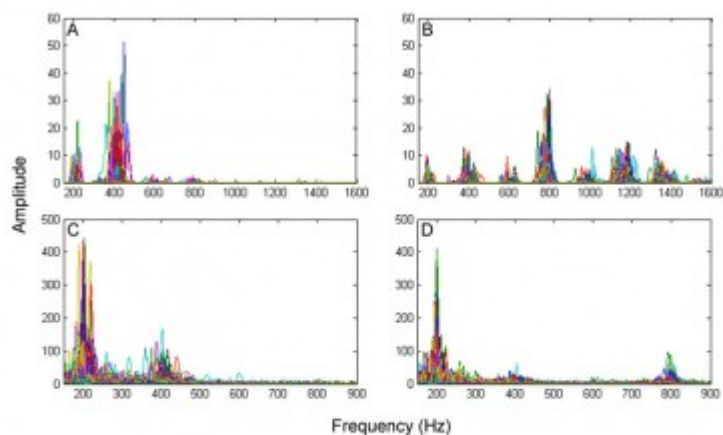


Illustration 7. Speech spectra from patient 5 showing frequency differences between words and response of the interferometer compared to the microphone. A and B show the microphone-detected frequency spectra of words "boot" and "light", respectively. C and D show the interferometer-detected frequency spectra of words "boot" and "light", respectively.

Illustration 8

Illustration 8

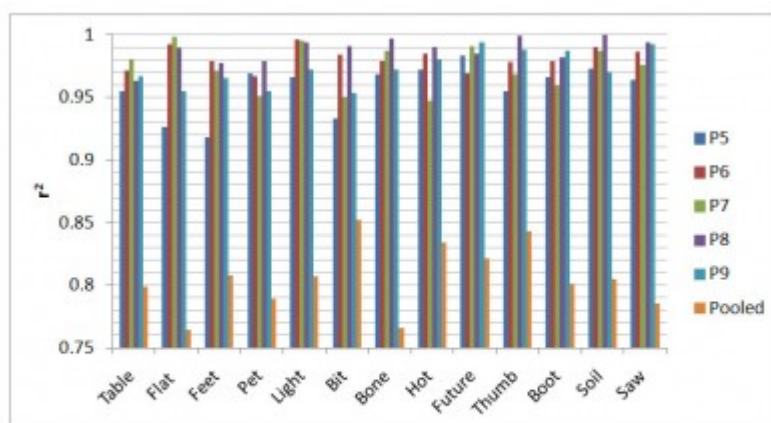


Illustration 8. Comparison of leave-one-out cross-validation correlations for predicted versus actual %BrAC from analysis of interferometer-recorded speech. Individual correlations were found with $r^2 > 0.91$.

Illustration 9

Illustration 9

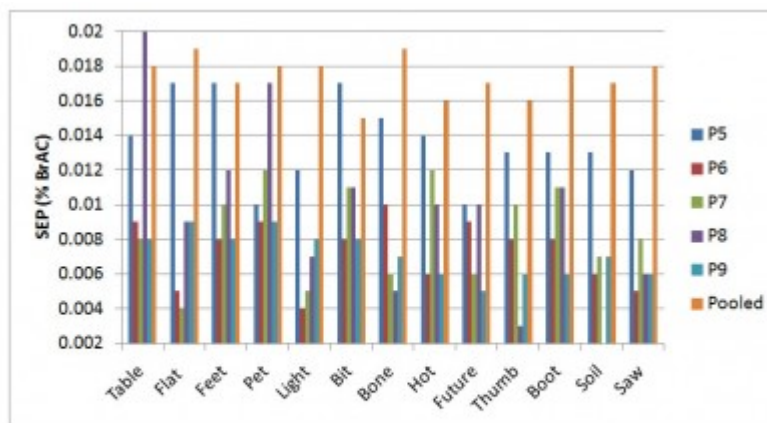


Illustration 9. Comparison of SEP from leave-one-out cross-validation for predicted versus actual %BrAC analysis of interferometer-recorded speech. The SEP for individual measurements was < 0.020 % BrAC.

Illustration 10

Illustration 10

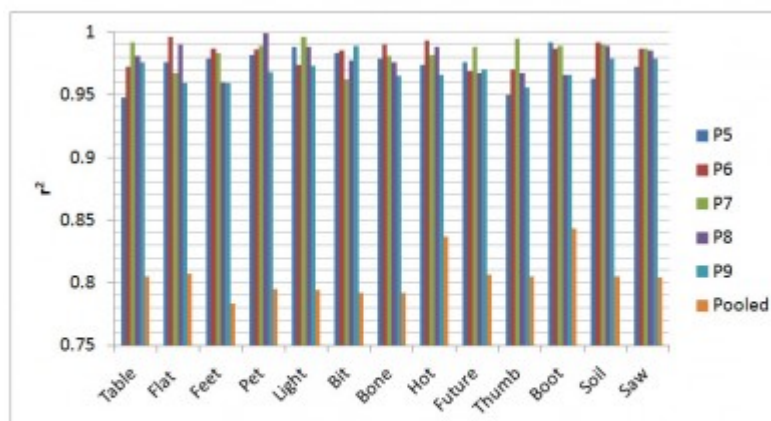


Illustration 10. Comparison of leave-one-out cross-validation correlations for predicted versus actual %BrAC from analysis of microphone-recorded speech. Individual correlations were found with $r^2 > 0.94$.

Illustration 11

Illustration 11

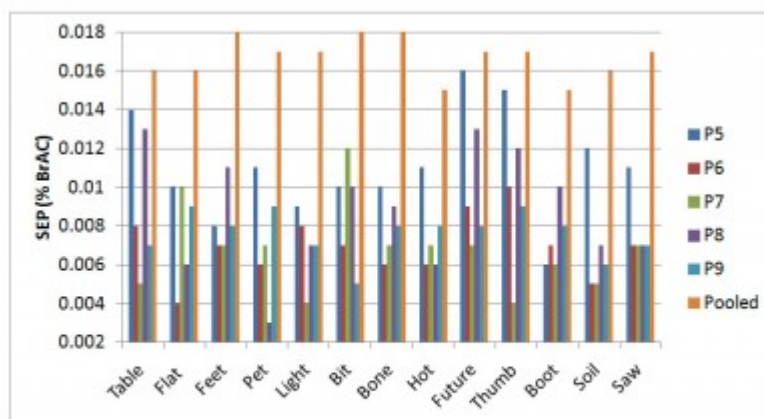


Illustration 11. Comparison of SEP from leave-one-out cross-validation for predicted versus actual %BrAC analysis of microphone-recorded speech. The SEP for individual measurements was < 0.016 % BrAC.